

Received August 22, 2019, accepted September 2, 2019, date of publication September 23, 2019, date of current version December 17, 2019.

Digital Object Identifier 10.1109/ACCESS.2019.2943156

# Research on Relativity of Flow Rate Distribution Inside the Rotor Domain for a Large-Scale Air-Cooled Turbo-Generator

SHUYE DING<sup>1</sup>, XIN JIANG<sup>1</sup>, ZHENJIANG LI<sup>1,2</sup>, AND ZHENGHUI LI<sup>1,2</sup>

<sup>1</sup>School of Electrical and Automation Engineering, Nanjing Normal University, Nanjing 210023, China

<sup>2</sup>Nanjing Intelligent High-end Equipment Industry Research Institute, Nanjing 210013, China

Corresponding author: Shuye Ding (dingshuye@163.com)

This work was supported in part by the National Natural Science Foundation of China under Grant 51977112, in part by the Province Natural Science Foundation of Jiangsu under Grant BK20191370, and in part by the Graduate Science and Innovation Projects in Jiangsu Province under Grant KYCX19\_0805.

**ABSTRACT** The main objective of this paper is to elucidate the effect of rotor end structures of a large-scale air-cooled turbo-generator on the flow rate distribution and fluid flow pattern in the rotor domain. A 350 MW fully air-cooled turbo-generator is taken as an example. Based on the original ventilation structure, two optimization schemes of adding wind deflectors and small fans to the end of the rotor are proposed. The finite volume method is used to solve the fluid field in the generator with different rotor end structures. The air volume distribution in each wind area of the generator is taken as the basis for checking the accuracy of the calculation. Under different schemes, the wind path direction, flow rate and fluid velocity distribution in the radial ventilation ducts, subslots and crescent slots of the rotor are compared and analyzed. The effects of these schemes on the overall flow rate distribution and the fluid parameter distribution characteristics in each rotor ventilation ducts are determined.


**INDEX TERMS** Air-cooled turbo-generator, finite volume method, fluid field, rotor, ventilation structure.

## I. INTRODUCTION

Large-scale thermal power units have been widely used in China's generator sets due to their high energy conversion efficiency and good system stability [1]. However, the bottleneck of the capacity improvement for the turbo-generator depends on reasonable ventilation structure and cooling design [2]. The subslot ventilation structure is commonly adopted for the rotor of air-cooling turbo-generators. As a consequence, the fluid flow inside the rotor becomes very complicated. Nevertheless, the cooling performance of the rotor plays a key role in the safe and stable operation of the turbo-generator. Therefore, it is necessary to accurately simulate the fluid flow in the rotor ventilation ducts of the high-power fully air-cooled turbo-generator. Moreover, it is also important to explore the influence of different rotor cooling structures on the flow rate distribution and fluid flow pattern in the generator. A large amount of research has been conducted to study the fluid field and temperature field [3], [4] of

the generator by using the finite element method [5]–[7] and the finite volume method [8]–[11]. To simplify the difficulty of modeling and reduce the calculation time, the two-dimensional finite element method is commonly used to analyze the temperature field of the generator [12]. However, the two-dimensional calculation model cannot accurately represent the fluid flow characteristics in the calculation domain. Furthermore, it is difficult to simulate the influence of axial ventilation on the temperature distribution of the generator. Therefore, a three-dimensional calculation model is a better choice for simulating the fluid field and temperature field distribution in the generator domain. For instance, the sensitivity of the generator cooling performance has been studied, and the temperature distribution of the cooling system was predicted numerically [13]. However, an equivalent model is used to reduce the complexity of the stator winding structure. Consequently, the accuracy of the fluid field distribution in the end region of the generator is decreased. Therefore, it is necessary to model the end winding accurately.

In a study on the heating and cooling of air-cooled turbo-generators, Han et al. investigate the effect of different

The associate editor coordinating the review of this manuscript and approving it for publication was Huiqing Wen .

cooling media [14] and cooling medium parameters [15] on the fluid velocity and temperature distribution in the end region of an air-cooled turbo-generator. In [16], the flow-heat coupling model of an air-cooled turbo-generator is solved by the finite element method, and the influence of the copper shield structure on the overall temperature rise of the generator is revealed. Li et al. calculate and analyze the fluid field and temperature field in the rotor [17] and the end regions [18] of a turbo-generator in detail, promoting the development of air-cooled turbo-generator rotor cooling technology. Nevertheless, the abovementioned studies revolve around the analysis of fluid field and temperature field in the local area of an air-cooled turbo-generator. Few studies have focused on the influence of the rotor ventilation structure on the flow rate distribution in the rotor domain.

In this paper, the 350 MW air-cooled turbo-generator is taken as an example. Two optimization schemes are proposed to improve the ventilation for the end structure of the rotor. Based on the basic assumptions, the mathematical and physical models of the ventilation system in 1/4 multi-wind zone of the generator are set up. Then, the fluid field of the generator with different rotor structures are calculated using the finite volume method. The effects of flow rate and velocity spatial distribution in the rotor axial and radial air ducts for different end structures of the rotor are compared and analyzed. The results confirm that the cooling air flow rate in the rotor region can be significantly increased by adding a small fan under the rotor retaining ring. Furthermore, adding wind deflectors between the windings at the end of the rotor has an obvious effect on the flow rate distribution of the adjacent rotor subslots.

## II. ESTABLISHMENT OF PHYSICAL MODEL AND MATHEMATICAL MODEL

### A. PHYSICAL MODEL AND BASIC ASSUMPTIONS

#### 1) GENERATOR VENTILATION STRUCTURE

The generator studied in this paper adopts a fully air cooling and self-ventilating cooling mode; the wind path of the ventilation structure is shown in Fig. 1.

The air cooled by the cooler is divided into two parts to enter the generator for cooling. One part of the cooling air directly enters the air inlet of the five stator straight sections that is separated by the ring plate of generator shell and then flows in a half-circle along the stator radial ventilation ducts on the back. The cooling air enters the air gap along the stator ventilation ducts because the upper part of the wind zone corresponding to the stator straight-line inlet is blocked by the baffle.

Another part of the cooling air enters through the air inlets of the wind paths at both ends of the stator straight section and then cools the generator via three pathways. Two of the paths flow into the air gap along the axis after cooling the stator end windings and the rotor core, separately. The rest of the air enters the casing after cooling the end surface of the stator straight section along the gap at the stator finger plate.

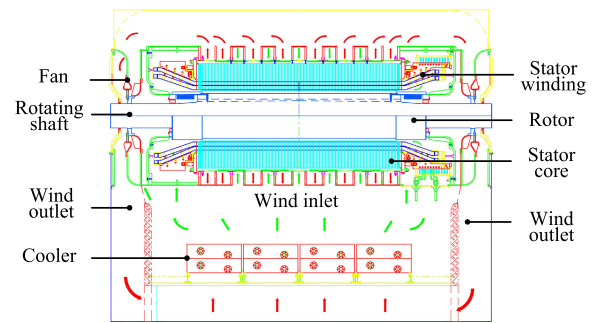


FIGURE 1. Schematic diagram of the ventilation cooling system.

The upper part of the stator straight section is separated into eight air outlets by the ring plate of the generator shell. After cooling the inside of the generator, the hot air enters the upper area of the generator shell and then flows to the end area of the generator, and finally, it is forced and removed by the fan at the end of the generator. At this point, self-circulation is completed.

#### 2) BASIC ASSUMPTIONS OF THE MODEL

The 350 MW generator studied in this paper is considered to adopt the self-ventilation method of fully air cooling, and its ventilation structure is extremely complex. Therefore, for a reasonable simplification of the solution procedure, the following basic assumptions are made in the model [19]:

- 1) The Reynolds number of the fluid is very large in the internal generator, and the fluid is turbulent; therefore, the standard  $k-\varepsilon$  model is used to calculate the fluid field of the generator.
- 2) The fluid velocity in the solution domain is lower than the sound velocity, so the generator fluid is treated as an incompressible fluid.
- 3) Since the fluid field in the generator is solved when the fluid flow is stable, that is, the flow is constant, the influence of time on solving the governing equation is not considered.
- 4) The buoyancy and gravity of the fluid in the ventilation ducts is ignored.
- 5) The influence of the channel steel in the stator ventilation duct on the fluid field is ignored.

#### 3) PHYSICAL MODEL OF THE SOLVING DOMAIN

Due to the symmetry of generator ventilation structure studied in this paper, half of the axial section and half of the circumferential section are selected respectively, that is, 1/4 of the fluid domain of the whole machine is chosen as the calculation solution domain, as shown in Fig. 2a).

Fig. 2b) shows the fluid domain of the generator rotor. The rotor rotates in the counterclockwise direction as viewed axially from the fan side. The model adopts the subslot ventilation cooling system, the lower end of the rotor slot is the subslots for ventilation. The rotor winding has radial ventilation holes that are composed of 6 end radial ventilation

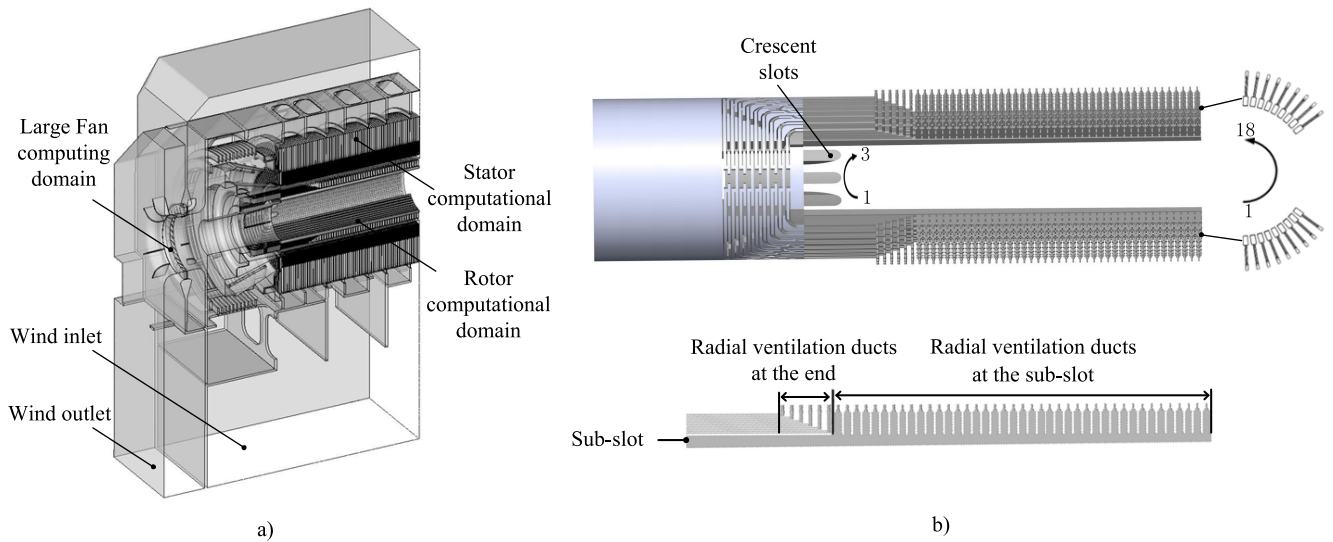


FIGURE 2. The computational domain. (a) The computational solution domain. (b) The rotor fluid domain.

ducts and 41 subslot radial ventilation ducts. In addition to the axial and radial ventilation ducts, the characteristics of the end retaining rings and crescent slots are also taken into account at the end of the rotor model.

### B. MATHEMATICAL MODEL

In the generator, the multidimensional flow of the fluid should follow the laws of conservation of physics, mainly including the laws of mass conservation and momentum conservation. The corresponding governing equations are as follows:

The fluid in the generator studied in this paper is an incompressible fluid, and its mass conservation equation can be described as [20]–[22]:

$$\frac{\partial u}{\partial x} + \frac{\partial v}{\partial y} + \frac{\partial w}{\partial z} = 0. \quad (1)$$

where  $u$ ,  $v$ , and  $w$  are the components of  $\mathbf{V}$  in the  $x$ -axis,  $y$ -axis, and  $z$ -axis directions.

The equation of momentum conservation is [22], [23]:

$$\begin{cases} \rho \frac{du}{dt} = -\frac{\partial p}{\partial x} + \rho X + \mu \Delta u \\ \rho \frac{dv}{dt} = -\frac{\partial p}{\partial y} + \rho Y + \mu \Delta v \\ \rho \frac{dw}{dt} = -\frac{\partial p}{\partial z} + \rho Z + \mu \Delta w \end{cases} \quad (2)$$

where  $p$  is the fluid pressure and  $\mu$  is the dynamic viscosity coefficient.

Due to the complex ventilation structure of the generator, the Reynolds number of the air in the generator is greater than the critical value when it reaches a stable operating state, namely, the fluid is in the turbulent motion state; therefore, the most widely used standard  $k$ - $\varepsilon$  turbulence calculation model is adopted to simulate the turbulent flow. The Boltzmann equation with the kinetic energy of turbulence

$k$  and diffusion factor  $\varepsilon$  is used in the turbulence model as follows [24]:

$$\frac{\partial(\rho k)}{\partial t} + \frac{\partial(\rho k u_i)}{\partial x_i} = \frac{\partial}{\partial x_j} \left[ \left( \mu + \frac{\mu_t}{\sigma_k} \right) \frac{\partial k}{\partial x_j} \right] + G_k + G_b - \rho \varepsilon + Y_M + S_K. \quad (3)$$

$$\frac{\partial(\rho \varepsilon)}{\partial t} + \frac{\partial(\rho \varepsilon u_i)}{\partial x_i} = \frac{\partial}{\partial x_j} \left[ \left( \mu + \frac{\mu_t}{\sigma_\varepsilon} \right) \frac{\partial \varepsilon}{\partial x_j} \right] + C_{1\varepsilon} \frac{\varepsilon}{k} (G_k + C_{3\varepsilon} G_b) - C_{2\varepsilon} \rho \frac{\varepsilon^2}{k} + S_\varepsilon. \quad (4)$$

where  $\rho$  is the fluid density,  $x_i$ , and  $x_j$  are the generation rates of the turbulence,  $C_{1\varepsilon}$ ,  $C_{2\varepsilon}$ , and  $C_{3\varepsilon}$  are empirical coefficients, and  $\sigma_k$  and  $\sigma_\varepsilon$  are Prandtl numbers.

### C. BOUNDARY CONDITIONS

According to the wind path structure and fluid flow characteristics of the air-cooled turbo-generator, the boundary conditions of the computational solution domain are as follows:

1) The boundary conditions of the pressure inlet and pressure outlet are adopted respectively at the inlet and outlet of the wind path, and the pressure values are set to 1 atm, namely, 101325 Pa.

2) The axis central section has symmetrical boundary conditions, and the other sections have periodic boundary conditions.

3) The rated speed of the rotor and the fan are the same, while the angular velocity is set to 314 rad/s. The planes between the dynamic and static regions are defined as the ‘interface’.

## III. NUMERICAL ANALYSIS OF THE CALCULATION OF THE ORIGINAL SCHEME

To verify and analyze the fluid evolution law and velocity distribution characteristics in the calculation domain, the generator model of the original structure is taken as the

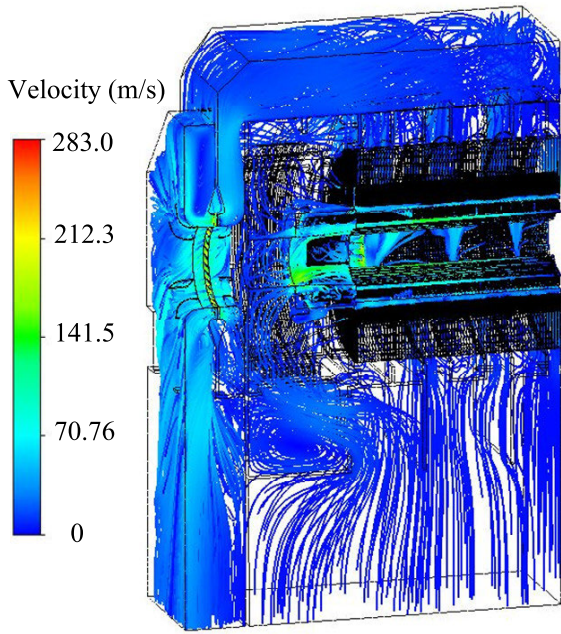


FIGURE 3. The velocity trace in the computational domain.

research object, and the velocity trace map in the calculation domain shown in Fig. 3 is given.

As shown in Fig. 3, the cooling air enters from the inlets of the wind path, and then, the flow path for cooling the generator is consistent with that described above. It is clear that the part of the cooling air entering the rotor cools the end of the rotor and then flows into the stator and rotor air gap through the crescent slot. The other part enters through 12 supplementary vents and subslots at the end of the rotor and then enters into the air gap through 6 end radial ducts and 41 straight segments radial ducts after flowing along the axial direction of the rotor. The fluid velocity distribution in each part of the computational domain is not uniform. Compared with that in the cavity region, the fluid velocity in the rotor and fan region is relatively high. The fan is the power component of the whole ventilation system of the generator so that the wind speed at this location is relatively high, which is consistent with the actual situation.

**IV. STRUCTURAL OPTIMIZATION DESIGN AND ANALYSIS OF CALCULATION RESULTS**

**A. SUMMARY OF ROTOR STRUCTURE OPTIMIZATION**

In the same type of generators, a baffle is usually added between the pole ends of the rotor to improve the aeration asymmetry between the rotor poles. To evaluate the influence of wind deflectors between the rotor end windings on the distribution of the overall air volume and cooling air volume in each wind duct of the rotor, this paper proposes scheme A for the structure of the end of the rotor, namely, the addition of two wind deflectors at each pole of the end of the rotor. Fig. 4a) shows the specific installation position and shapes of the wind deflectors. It is observed that the installation

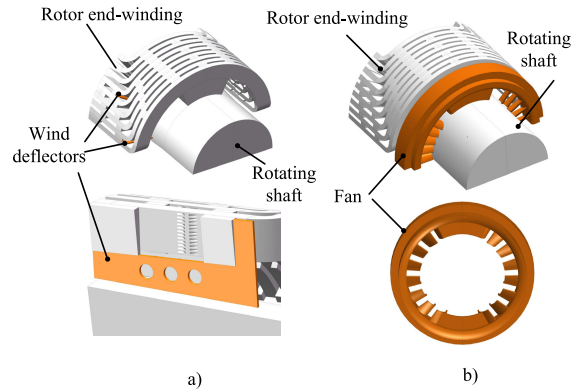


FIGURE 4. Rotor optimization model diagram. (a) Scheme A. (b) Scheme B.

positions of the wind deflectors are not symmetrical and are both located on the windward side of the pole, with one between the No. 4 and No. 5 windings and the other between the No. 8 and No. 9 windings.

In view of the rotation effect of the rotor, it is necessary to add the structural parts in the rotor region to change the structure of the wind path and the flow rate distribution within a certain range. To this end, this paper proposes scheme B shown in Fig. 4b), namely, the addition of a small fan under the end retaining ring of the rotor based on the original scheme.

**B. ANALYSIS OF CALCULATED AND DESIGNED VALUES**

The finite volume method is used to solve the three-dimensional fluid flow model during stable operation of the generator. To verify the correctness of the solution method, Table 1 shows the flow rate distribution of each region in the calculation domain. The four stator straight section air outlets separated by the ring plate of generator shell are numbered from the left to the right as the hot air zones of Nos. 1, 2, and 3 (the first two air outlets are numbered as the hot air zone of No. 1), and three stator straight section air inlets are respectively defined as the cold air zones of Nos. 1, 2, and 3.

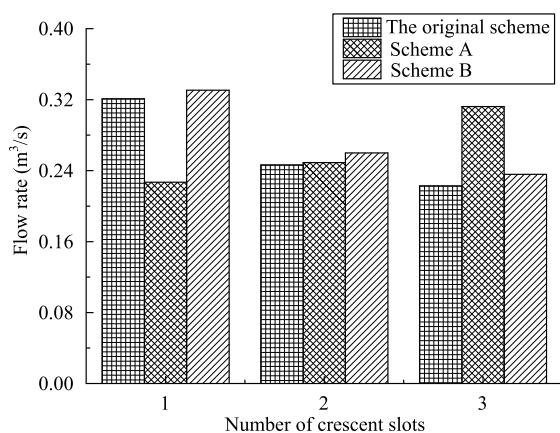
Comparison of the calculated and designed values of the flow rate in each wind area of the generator in Table 1 shows that the maximum error of the wind volume in each area of the original scheme is 8.45%. The calculated results are consistent with the designed values, meeting the accuracy requirements and verifying the accuracy of the calculated results as well as the validity of the solution method.

By comparing the flow rate distribution in each region under the three schemes, it is found that the total air volume in scheme A is significantly lower than that in the other schemes. With the exception of the rotor fluid domain, the errors between the calculated and designed air volumes in other areas of scheme A are obviously larger than those in the original scheme. This is because the wind deflectors can improve the local wind volume distribution of the rotor, and it acts as the wind resistance in the overall ventilation



**TABLE 1.** Comparison of flow designed value and calculated value in each region of the generator.

Zones	Designed value(m <sup>3</sup> /s)	Calculated value					
		Original scheme (m <sup>3</sup> /s)	Error	Scheme A (m <sup>3</sup> /s)	Error	Scheme B (m <sup>3</sup> /s)	Error
Total wind flow	22.02	21.69	-1.50%	20.65	-6.22%	22.29	1.23%
No.1 hot wind zone	9.82	8.99	-8.45%	8.45	-13.95%	9.22	-6.11%
No.2 hot wind zone	5.35	5.32	-0.56%	5.06	-5.42%	5.47	2.24%
No.3 hot wind zone	5.35	5.36	0.19%	5.12	-4.30%	5.50	2.80%
Rotor	4.83	5.05	4.55%	5.09	5.38%	5.39	11.59%
No.1 cold wind zone	4.35	4.17	-4.14%	3.93	-9.66%	4.18	-3.91%
No.2 cold wind zone	4.34	4.12	-5.07%	3.86	-11.06%	4.12	-5.07%
No.3 cold wind zone	2.17	1.99	-8.29%	1.91	-11.98%	2.04	-5.99%

**FIGURE 5.** Flow rate distribution in the crescent slots.

system, making the overall flow rate lower than expected. In scheme B, the rotor is affected by the small fan pumping, so the cooling air volume that flows into the rotor fluid area is improved, and the differences between the calculated and designed values of the air flow rate in each cold and hot air area are reduced.

### C. CALCULATION AND ANALYSIS OF FLUID FLOW

The total air flow rate that cools the rotor enters through the inlet of the rotor end retaining ring. After cooling the rotor, this air enters the air gap through the crescent slot and the radial ventilation ducts of the rotor.

Fig. 5 shows the flow rate distribution of the crescent slots of the rotor under each scheme. It is observed that the windward and leeward sides generated by the rotation of the rotor make the air flow rate distribution of the three crescent slots uneven in each scheme. For scheme B, it is observed that the air flow rate distribution trend of the crescent slot is consistent with that of the original scheme. The air flow in the No. 3 slot on the windward side is the smallest, while that in the No. 1 slot on the leeward side is the largest. Scheme A is affected by the wind deflectors between the windings of the rotor end so that the distribution of the air flow rate in each crescent slot in this scheme is exactly opposite to those in the former two schemes.

Regarding the total air volume of the three crescent slot, the total air volume of the crescent slot in the original scheme is the same as that in scheme A, with both of these equal to 0.79 m<sup>3</sup>/s. In scheme B, the small fan structure at the end of the rotor maximizes the total air output of the crescent slot, which is 0.827 m<sup>3</sup>/s.

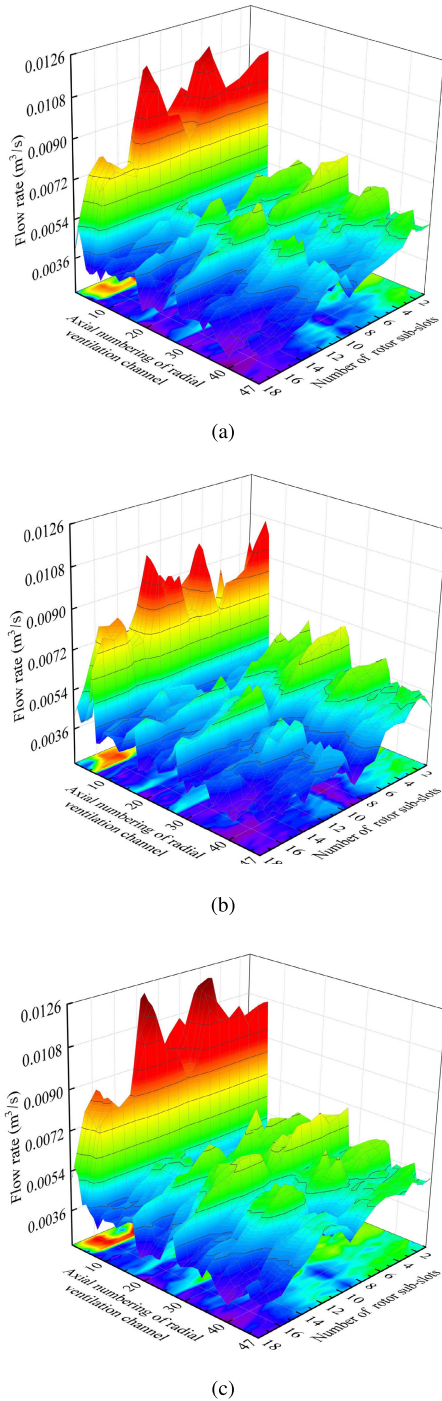
In this paper, the 1/4 region of the whole machine is selected as the calculation domain, and there are 18 rotor subslots in the rotor fluid domain. Each rotor winding has 6 radial ventilation ducts at the end and 41 radial ventilation ducts at the subslots, for a total of 846 rotor radial ventilation ducts.

Fig. 6 shows the air flow rate distribution of the rotor radial ventilation ducts under different schemes. It can be seen that the distribution trend of air flow rate in the radial ventilation ducts of the rotor is almost the same in different schemes. In the circumferential direction, due to the rotation of the rotor, the flow rate distribution of the radial ventilation ducts has a clear boundary between the windward and leeward sides.

Since there are 12 air supply holes at the end of each winding, and each radial ventilation duct at the end is connected with two air supply holes, the air flow rate of the radial ventilation ducts at the end is larger than that of the subslot section in the axial direction.

Fig. 7 shows the air flow rate distribution of each rotor subslot under different optimized schemes. It is seen that the flow rate distribution in the subslot under each scheme is similar to the circumferential distribution trend of each radial ventilation duct as shown in Fig. 6. Due to the rotation of the rotor, the flow rate distribution in the subslots around circumference is not uniform, and the air flow rate into the subslots on the windward side of each scheme is smaller than that on the leeward side.

The distribution of the air flow rate in each subslot on the windward side for scheme A with wind deflectors added between the windings is more uniform than that in the original scheme, while the air flow rate of the leeward side subslots in both schemes is unevenly distributed. The reason is because the wind deflectors in scheme A are located between the No. 13 and No. 14 subslots and between the No. 17 and No. 18 subslots (between the No. 4 and No. 5 windings and



**FIGURE 6. Flow rate distribution in rotor radial ventilation ducts. (a) Original scheme. (b) Scheme A. (c) Scheme B.**

the No. 8 and No. 9 windings on the windward side), but there are no wind deflectors on the leeward side; as the result, the wind deflector plays a more significant role in improving the air flow rate distribution of the adjacent sub-slots.

With the exception of the individual rotor sub-slots, the air flow rates of each subslot in the original scheme and scheme A are smaller than those in scheme B with a small rotor fan, but compared with that in the original scheme, the addition

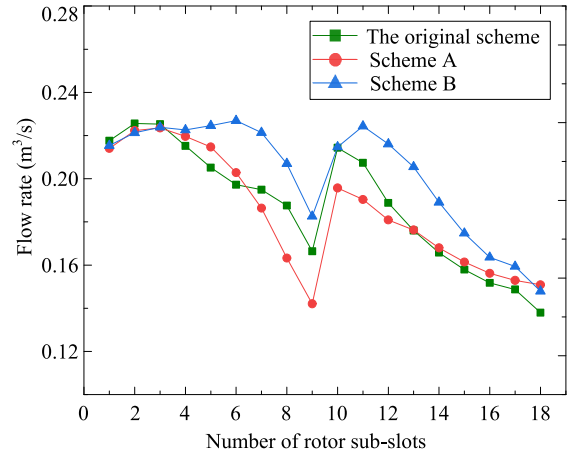


**FIGURE 7. Flow rate distribution in the rotor winding sub-slots.**

of the small rotor fan in scheme B has little effect on the air flow rate distribution trend of the sub-slots around the circumference.

**D. CALCULATION AND ANALYSIS OF FLUID FLOW VELOCITY**

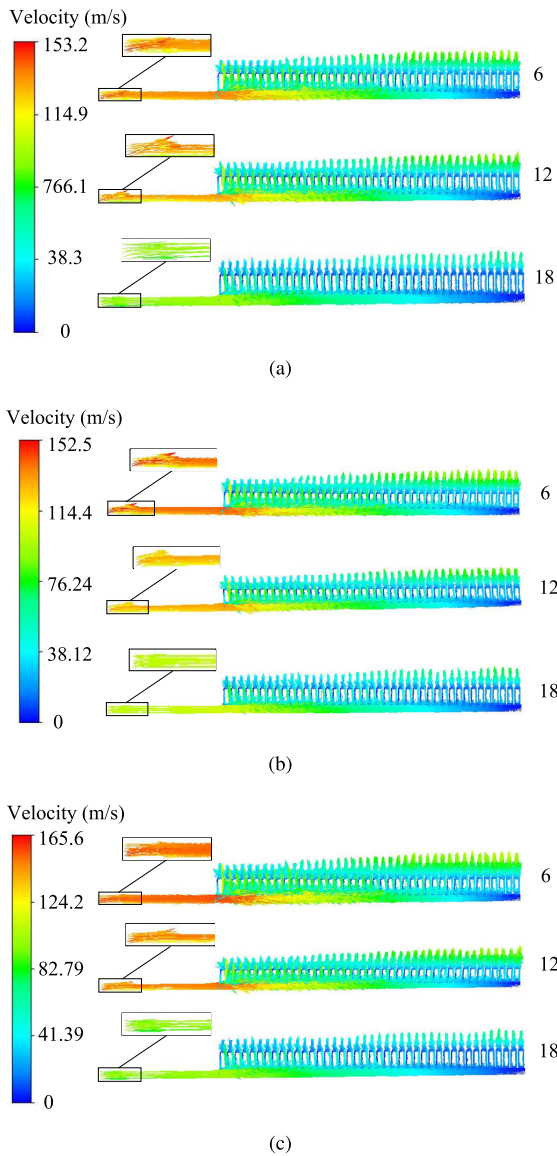
To clarify the laws governing the cooling air flow in the rotor sub-slots in more detail, the rotor sub-slots Nos. 6, 12 and 18 are taken as the research object, and the velocity vectors of the sub-slots under various schemes are shown in Fig. 8.

According to the figure, the axial fluid velocity distribution trends in the rotor sub-slots obtained using the three schemes are similar, and this is also observed for the radial fluid velocity distribution trends. Additionally, the flow rate in scheme B is significantly larger than that for the original scheme and for scheme A. As no radial ventilation duct is directly connected to the end of the sub-slots, the fluid velocity in the sub-slots increases gradually. On the other hand, the radial ventilation ducts are connected to the straight section of the rotor sub-slots, making the wind path in the subslot complicated and gradually decreasing the velocity.

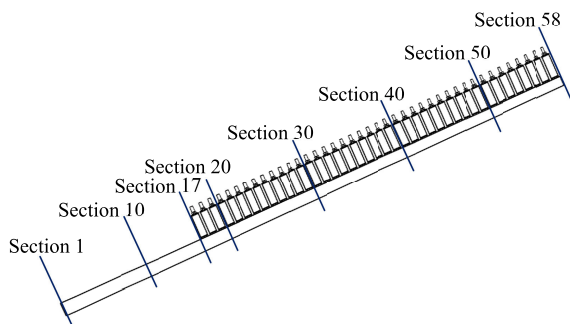
To study the variation trend of the axial fluid flow in the subslot, the sections are placed at intervals of 50 mm from the inlet of the wind path at the end of the rotor subslot along the axis extension direction to ensure the existence of a section between the two adjacent rotor radial ventilation ducts, as shown in Fig. 9.

Fig. 10 shows the average velocity distribution of the cooling air in subslot Nos. 6, 12 and 18 under different schemes. Overall, the average velocity of each section in the axial direction first increases and then decreases, similar to the velocity vector diagram of each subslot presented in Fig. 8.

By comparison of the results for scheme A with those obtained using the original scheme, it is observed that the average velocities of the sections in the No. 6 and No. 12 sub-slots are slightly different, while those of the sections in the No. 18 subslot in the scheme A are larger because the wind deflectors between the No. 17 and No. 18 sub-slots in scheme

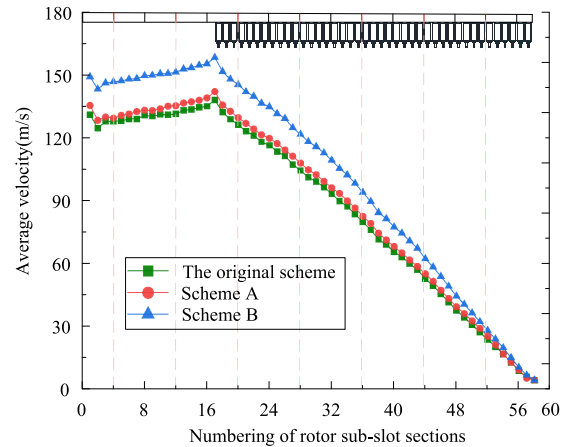


**FIGURE 8.** Velocity vector diagram of the rotor slots and the overall picture of the incident port. (a) Original scheme. (b) Scheme A. (c) Scheme B.

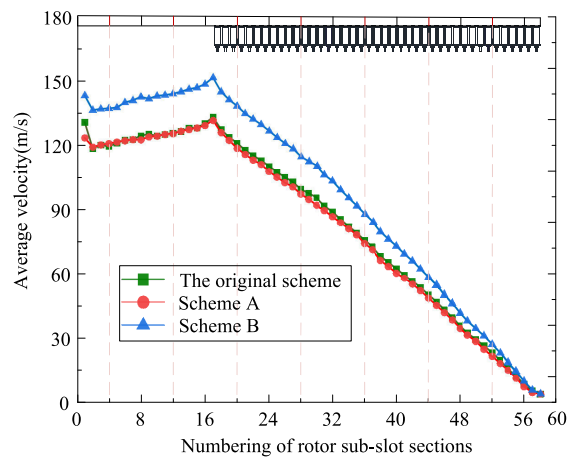


**FIGURE 9.** Schematic diagram of the cross-section of the rotor slots.

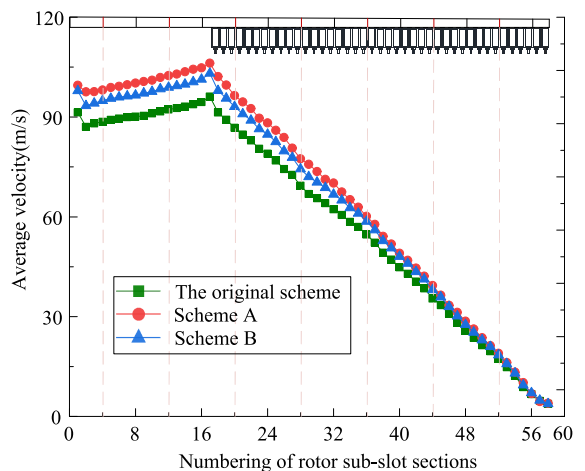
A improved the air passage at the air supply inlet of the straight section of the adjacent subslots. Compared with the original scheme, the average velocity of each subslot section



(a)



(b)



(c)

**FIGURE 10.** Average velocity of a cross-section of the rotor slots. (a) Original scheme. (b) Scheme A. (c) Scheme B.

in the scheme B is larger than that in the original scheme, which indicates that the increase in the rotor small fan at the rotor end has a significant effect on increasing the fluid flow velocity in the circumferential rotor slots.

## V. CONCLUSION

In this paper, a 350 MW air-cooled turbo-generator is taken as an example, and two optimization schemes are proposed for its rotor end structure. A three-dimensional physical model is established, and then, the fluid flow performance of the generator is studied by using the finite volume method. The conclusions are as follows:

1) The air volume distribution in each region is calculated, and the calculated results are largely in agreement with the design values. Adding a small fan under the rotor retaining ring balances the air flow rate distribution in the whole region of the generator, while the added wind deflectors between the windings are equivalent to the wind resistance in the whole wind path, and do not perform well in the overall air flow rate distribution of the machine.

2) Compared with that in the original scheme, the addition of wind deflectors between the rotor end windings changes the distribution trend of the air volume in each crescent slot, but this has little effect on the total air flow rate in the crescent slots. Adding a small fan structure for the rotor has no effect on the distribution trend of the air flow rate in each crescent slot, but it can significantly increase the total air volume in the crescent slot region.

3) Adding the wind deflectors between the end windings of the rotor improves the uniformity of the air flow rate distribution in the adjacent subslots, while adding a small fan at the end of the rotor improves the fluid flow velocity in the circumferential rotor subslots and the total air flow rate in the rotor, but it has little effect on the distribution trend of the air flow rate in each part of the rotor.

4) By synthetically measuring the total air volume, the air distribution in each region and the fluid evolution in the rotor, scheme B can significantly improve the ventilation performance of the generator.

## REFERENCES

- [1] L. Yu, X. Jin, Z. Li, Y. Xiong, and W. Huang, "An intelligent scheduling approach for electric power generation," *Chin. J. Electron.*, vol. 27, no. 6, pp. 1170–1175, Nov. 2018.
- [2] K. Ide, K. Hattori, K. Takahashi, K. Kobashi, and T. Watanabe, "A sophisticated maximum capacity analysis for large turbine generators considering limitation of temperature," *IEEE Trans. Energy Convers.*, vol. 20, no. 1, pp. 166–172, Mar. 2005.
- [3] M. Mohammadi, H. Ansari, P. Bahemmat, and A. A. Kharamani, "Thermal analysis of the rotor of large air-cooled turbo generators," in *Proc. 3rd Conf. Therm. Power Plants (CTPP)*, Oct. 2011, pp. 1–6.
- [4] X. Bin, G. Gu, R. Lin, Z. Li, D. Fu, R. Cao, S. Guo, and J. Gao, "Studies on the structure of radial ventilation channel to improve the cooling capacity of large turbo generator stator," in *Proc. 17th Int. Conf. Elect. Mach. Syst. (ICEMS)*, Oct. 2014, pp. 354–357.
- [5] L. Wang and W. Li, "Assessment of the stray flux, losses, and temperature rise in the end region of a high-power turbogenerator based on a novel frequency-domain model," *IEEE Trans. Ind. Electron.*, vol. 65, no. 6, pp. 4503–4513, Jun. 2018.
- [6] R. Krok, R. Miksiewicz, and W. Mizia, "Modeling of temperature fields in turbo generator rotors at asymmetrical load," in *Proc. Int. Conf. Elect. Mach.*, 2000, pp. 1005–1009.
- [7] S. Ding, G. Cui, Z. Li, and T. Guan, "Fluid and thermal performance analysis of PMSM used for driving," *Heat Mass Transf.*, vol. 52, no. 3, pp. 571–579, Jun. 2016.
- [8] J. Han, B. Ge, and W. Li, "Influence of magnetic permeability of the Press plate on the loss and temperature of the end part in the end region of a turbogenerator," *IEEE Trans. Ind. Electron.*, vol. 66, no. 1, pp. 162–171, Jan. 2019.
- [9] W. Yoo, S. Jeon, C. Son, J. Yang, D. Ahn, S. Kim, K. Hwang, and S. Ha, "Full surface heat transfer characteristics of rotor ventilation duct of a turbine generator," *Appl. Therm. Eng.*, vol. 94, pp. 385–394, Feb. 2016.
- [10] S. Ding, J. Liu, and L. Zhang, "Fan characteristics of the self-support components of rotor ends and its performance matching," *Int. J. Heat Mass Transf.*, vol. 108, pp. 1917–1923, May 2017.
- [11] L. Weili, H. Jichao, Z. Xingfu, and L. Yong, "Calculation of ventilation cooling, three-dimensional electromagnetic fields, and temperature fields of the end region in a large water–hydrogen–hydrogen-cooled turbogenerator," *IEEE Trans. Ind. Electron.*, vol. 60, no. 8, pp. 3007–3015, Aug. 2013.
- [12] W. Li, P. Wang, D. Li, X. Zhang, J. Cao, and J. Li, "Multiphysical field collaborative optimization of premium induction motor based on GA," *IEEE Trans. Ind. Electron.*, vol. 65, no. 2, pp. 1704–1710, Feb. 2018.
- [13] G. Zhu, X. Liu, L. Li, H. Chen, W. Tong, and J. Zhu, "Cooling system design of a high-speed PMSM based on a coupled fluidic–thermal model," *IEEE Trans. Appl. Supercond.*, vol. 29, no. 2, Mar. 2019, Art. no. 0601405.
- [14] J. Han, B. Ge, D. Tao, and W. Li, "Calculation of temperature distribution in end region of large turbogenerator under different cooling mediums," *IEEE Trans. Ind. Electron.*, vol. 65, no. 2, pp. 1178–1186, Feb. 2017.
- [15] J. Han, B. Ge, D. Tao, and W. Li, "Influence of cooling fluid parameter on the fluid flow and end part temperature in end region of a large turbogenerator," *IEEE Trans. Energy Convers.*, vol. 31, no. 2, pp. 466–476, Jun. 2016.
- [16] H. Feiyang, H. Jichao, L. Weili, Z. Xingfu, Z. Yihuang, L. Yong, and G. Chunwei, "Influence of copper shield structure on 3-D electromagnetic field, fluid and temperature fields in end region of large turbogenerator," *IEEE Trans. Energy Convers.*, vol. 28, no. 4, pp. 832–840, Dec. 2013.
- [17] L. Weili, Z. Feng, and C. Liming, "Calculation of rotor ventilation and heat for turbo-generator radial and tangential air-cooling system," in *Proc. Int. Conf. Power Syst. Technol. (POWERCON)*, vol. 2, Aug. 1998, pp. 1030–1033.
- [18] L. Weili, H. Jichao, H. Feiyang, Z. Xingfu, Z. Yihuang, and L. Yong, "Influence of the end ventilation structure change on the temperature distribution in the end region of large water–hydrogen–hydrogen cooled turbogenerator," *IEEE Trans. Energy Convers.*, vol. 28, no. 2, pp. 278–288, Jun. 2013.
- [19] A. N. Bolicic, "Aerodynamics and heat transfer in electrical machine," *Tech. Rep.*, 1985.
- [20] L. Weili, G. Chunwei, and C. Yuhong, "Influence of rotation on rotor fluid and temperature distribution in a large air-cooled hydrogenerator," *IEEE Trans. Energy Convers.*, vol. 28, no. 1, pp. 117–124, Mar. 2013.
- [21] D. A. Staton and A. Cavagnino, "Convection heat transfer and flow calculations suitable for electric machines thermal models," *IEEE Trans. Ind. Electron.*, vol. 55, no. 10, pp. 3509–3516, Oct. 2008.
- [22] R. W. Lewis, P. Nithiarasu, and K. N. Seetharamu, *Fundamentals of the Finite Element Method for Heat and Fluid Flow*. Hoboken, NJ, USA: Wiley, 2004.
- [23] A. Masmoudi, S. Ding, and M. Wang, "Comparison investigation of fluid rheological characteristics effect on stator temperature field for large hydro-generator based on experiment," *COMPEL, Int. J. Comput. Math. Elect. Electron. Eng.*, vol. 34, no. 1, pp. 234–247, 2015.
- [24] Y. Zhang, J. Ruan, T. Huang, X. Yang, H. Zhu, and G. Yang, "Calculation of temperature rise in air-cooled induction motors through 3-D coupled electromagnetic fluid-dynamical and thermal finite-element analysis," *IEEE Trans. Magn.*, vol. 48, no. 2, pp. 1047–1050, Feb. 2012.



**SHUYE DING** was born in 1978. He received the B.S., M.S., and Ph.D. degrees in electrical machinery and appliance from the Harbin University of Science and Technology, Harbin, in 2001, 2004, and 2008, respectively.

He is currently a Professor with the School of Electrical and Automation Engineering, Nanjing Normal University, Nanjing, China. He is the author or coauthor of more than 80 published peer-reviewed articles and holds more than ten patents.

His research interests include synthesis physical fields of large electrical machines and theoretical study of special electrical machines.





**XIN JIANG** was born in Nantong, China, in 1995. He is currently pursuing the M.S. degree in electrical engineering with the School of Electrical and Automation Engineering, Nanjing Normal University, Nanjing, China. His research interest includes ventilation cooling, fluid, and thermal analysis on electrical machine.



**ZHENGHUI LI** was born in Yangzhou, China. He is currently pursuing the M.S. degree in electrical engineering with Nanjing Normal University, Nanjing, China. His research interest includes fluid and thermal analysis on large electrical machine.

...



**ZHENJIANG LI** was born in Lianyungang, China, in 1996. He is currently pursuing the M.S. degree in the Nanjing Normal University, Nanjing, China. His research interests include numerical calculation of temperature and fluid field in the electrical machine.